PNNL-15573

Pacific Northwest
National Laboratory
Operated by Battelle for the
U.S. Department of Energy

Experimental Study of Micron-Size Zero-Valent Iron Emplacement in Permeable Porous Media Using Polymer-Enhanced Fluids

M. Oostrom
T. W. Wietsma
M. A. Covert
V. R. Vermeul

December 2005

Prepared for the U.S. Department of Energy
under Contract DE-AC05-76RL01830

DISCLAIMER

This report was prepared as an account of work sponsored by an agency of the United States Government. Neither the United States Government nor any agency thereof, nor Battelle Memorial Institute, nor any of their employees, makes any warranty, express or implied, or assumes any legal liability or responsibility for the accuracy, completeness, or usefulness of any information, apparatus, product, or process disclosed, or represents that its use would not infringe privately owned rights. Reference herein to any specific commercial product, process, or service by trade name, trademark, manufacturer, or otherwise does not necessarily constitute or imply its endorsement, recommendation, or favoring by the United States Government or any agency thereof, or Battelle Memorial Institute. The views and opinions of authors expressed herein do not necessarily state or reflect those of the United States Government or any agency thereof.

PACIFIC NORTHWEST NATIONAL LABORATORY
operated by

BATTELLE
for the
UNITED STATES DEPARTMENT OF ENERGY
under Contract DE-AC05-76RL01830

Printed in the United States of America
Available to DOE and DOE contractors from the
Office of Scientific and Technical Information,
P.O. Box 62, Oak Ridge, TN 37831-0062;
ph: (865) 576-8401
fax: (865) 576-5728
email: reports@adonis.osti.gov

Available to the public from the National Technical Information Service,
U.S. Department of Commerce, 5285 Port Royal Rd., Springfield, VA 22161
ph: (800) 553-6847
fax: (703) 605-6900
email: orders@ntis.fedworld.gov
online ordering: http://www.ntis.gov/ordering.htm

 This document was printed on recycled paper.
(9/2003)

PNNL-15573

Experimental Study of Micron-Size Zero-Valent Iron Emplacement in Permeable Porous Media Using Polymer-Enhanced Fluids

M. Oostrom
T. W. Wietsma
M. A. Covert
V. R. Vermeul

December 2005

Pacific Northwest National Laboratory
Richland, WA 99354

Summary

At the Hanford Site, an extensive In Situ Redox Manipulation (ISRM) permeable reactive barrier was installed to prevent chromate from reaching the Columbia River. However, chromium has been detected in several wells, indicating a premature loss of the reductive capacity in the aquifer. One possible cause for premature chromate breakthrough is associated with the presence of high-permeability zones in the aquifer. In these zones, groundwater moves relatively fast and is able to oxidize iron more rapidly. There is also a possibility that the high-permeability flow paths are deficient in reducing equivalents (e.g., reactive iron) required for barrier performance. The current barrier reductive capacity can be enhanced by adding micron-scale zero-valent iron to the high-permeability zones within the aquifer.

The potential emplacement of zero-valent iron (Fe^0) into high-permeability Hanford sediments (Ringold Unit E gravels) using shear-thinning fluids containing polymers was investigated in three-dimensional wedge-shaped aquifer models. Polymers were used to create a suspension viscous enough to keep the Fe^0 in solution for extended time periods to improve colloid movement into the porous media without causing a permanent detrimental decrease in hydraulic conductivity. Porous media were packed in the wedge-shaped flow cell to create either a heterogeneous layered system with a high-permeability zone between two low-permeability zones or a high-permeability channel surrounded by low-permeability materials. The injection flow rate, polymer type, polymer concentration, and injected pore volumes were determined based on preliminary short- and long-column experiments.

The flow cell experiments indicated that iron concentration enhancements of at least 0.6% (w/w) could be obtained using moderate flow rates and injection of 30 pore volumes. The aqueous pressure increased by as much as 25 KPa (~3.5 psi) during infiltration, but a decrease in hydraulic conductivity was not observed. The 0.6% amended Fe^0 concentration would provide approximately 20 times the average reductive capacity that is provided by the dithionite-reduced Fe(II) in the ISRM barrier.

Calculations show that the longevity of a 0.6% amended zero-valent iron zone will provide 2640 pore volumes of treatment before breakthrough is observed, assuming groundwater flowing through the treatment zone contains 8 mg/L oxygen, 60 mg/L nitrate, and 2 mg/L chromate, and assuming a complete reduction of these redox-reactive species. For instance, a 1-m-long Fe^0 amended zone with an average concentration of 0.6% w/w iron subject to a groundwater velocity of 1 m/day will have an estimated longevity of 7.2 years. To provide an example of comparable scale to that which would be required at the 100-D Area ISRM barrier site, a 10-m-long amended zone with an average concentration of 0.6 w/w % zero-valent iron, subject to a typical 100-D Area groundwater velocity of 0.3 m/day, would have an estimated longevity of 240 years.

The flow cell experiments conducted in this study indicated that in the downstream half of the flow cell the iron concentration stabilizes at about 0.6 % (w/w). These results suggest that additional research is needed in longer intermediate-scale flow cells to investigate how far from the injection well considerable iron enhancements can be obtained. For effective supplemental treatment of the 100-D Area ISRM barrier, a radial extent of treatment of approximately 5–7 m would be required. Flow cell experiments are also needed to provide direct measurement of the longevity of high-permeability zones amended with zero-valent iron. In these experiments, groundwater with representative dissolved oxygen, nitrate, and chromate concentrations would be allowed to move through the amended zones. Through sampling at various locations, oxygen, nitrate, and chromium concentration data would be collected. Results from these experiments should be compared with results from longevity calculations presented in this report. These experiments would also be useful for determining how groundwater displaces the emplaced viscous polymer solutions and to study how the injected polymer degrades over time.

Contents

Summary iii

1.0 Introduction 1.1

2.0 Materials and Methods 2.1

2.1 Porous Media 2.2
2.2 Zero-valent Iron Types 2.3
2.3 Polymers 2.3
2.4 Column Experiments 2.3
2.5 Flow Cell Experiments 2.4
2.6 Sample Analysis 2.6

3.0 Results and Discussion 3.1

3.1 Short-Column Experiments with 12/20 Accusand 3.1
3.2 Short-Column Experiments with Ringold-E Sediment 3.5
3.3 Long-column Experiments 3.7
3.4 Flow Cell Experiments 3.8

4.0 Summary 4.1

5.0 References 5.1

Appendix - Iron Concentrations for Experiments A.1

Figures

1 Hanford Site 100-D ISRM Barrier Location and Chromate Plume 1.2
2 100-D ISRM Well Chromate Concentrations and Borehole Locations Where Sediment Was Obtained for This Study 1.3
3 Experimental Setup of Flow Cell Experiment 2.4
4 Sampling Locations for Each of the Five Levels in the Flow Cell 2.5
5 Cross-Sectional View of the Outflow End of Flow Cell Experiment 1 ..... 2.5
6 Cross-Sectional View of the Outflow End of Flow Cell Experiment 2 ..... 2.5
7 Plan View of Flow Cell Experiment 1 with Location of High-Permeability Channel 2.6
8 H-200 Iron Suspension Injection at 0.05 cm/s with 0.02% SP after 30 Pore Volumes 3.1
9a Injection of S-3700 in 12/20 Accusand Using a 0.02% SP Suspension after 0, 0.5, and 1 Pore Volume 3.2
9b Injection of S-3700 in 12/20 Accusand Using a 0.02% SP Suspension at 0.02 cm/s after 3, 10, and 30 Pore Volumes 3.3
10a Injection of S-3700 in High-Permeabilty Ringold Material Using a 0.02% Slurry Pro Suspension at 0.02 cm/s after 0, 0.5, 1, and 3 Pore Volumes 3.6
10b. Injection of S-3700 in High-Permeability Ringold Material Using a 0.02% Slurry Pro Suspension at 0.02 cm/s after 10 Pore Volumes 3.7
11 Amended % Fe^0 as Function of Distance from Inlet for SP and AMPS Treatments 3.7
12 Top View of Failed Flow Cell Experiment Due to Fracturing of Upper Low-Permeability Layer 3.8
13 Excavated Surfaces for Sampling in Levels 2, 3, and 4 for Experiment 1 ..... 3.9
14 Excavated Surface for Level 2 with Inserted Samplers for Experiment 1 ..... 3.9
15 Excavated Surface for Level 2 with Inserted Samplers for Experiment 2 ..... 3.10
16 Amended % Fe^0 at all Five Levels as a Function of Distance from Injection Location (Experiment 1) 3.10
17 Amended % Fe^0 at All Five Levels as a Function of Distance from Injection Location (Experiment 2) 3.11

Tables

1 Overview of 20-cm Column Experiments 2.1
2 Amended Fe^0 Concentrations for 20-cm Column Experiments with 12/20 Accusand and S-3700 Iron 3.4
3 Amended Fe^0 Concentrations for 20-cm Column Experiments with Ringold E Sediment and S-3700 Iron 3.5

1.0 Introduction

At the Hanford Site, chromate-rich water leaked into the soil and contaminated the groundwater. In 1995, a plume of dissolved hexavalent chromium [Cr(VI)] was discovered along the Columbia River shoreline and in the 100-D Area. Between 1999 and 2003, an In Situ Redox Manipulation (ISRM) barrier was installed to prevent chromate from reaching the Columbia River. The ISRM technology involves creation of a treatment zone within an aquifer by injection of chemicals to alter the redox potential. At the Hanford Site, sodium dithionite, which is a strong reducing agent that reduces ferric iron [Fe(III)], related metals, and oxy-ions (Fruchter et al. 2000; Vermeul et al. 2002; Scezscody et al. 2004), has been used. The Hanford Site barrier consists of 65 injection wells spaced across a 680-m section near the Columbia River (Figure 1). Figure 1 shows Cr(VI) aqueous concentration contour lines for the first quarter of FY 2005. The reduction of ferric iron to ferrous [Fe(II)] iron provides the primary capacity to remove Cr(VI) from the groundwater as it flows through the treatment zone under natural flow conditions. Treatment of chromium contaminated groundwater occurs through reduction of chrome from the mobile hexavalent state to relatively immobile and less toxic trivalent state.

Initial field and laboratory tests indicated that the barrier shown in Figure 1 should have maintained its reductive capacity for approximately 20 years in the presence of < 2 mg/L chromate and dissolved oxygen in the groundwater. Szecsody et al. (2005) showed that the presence of a widespread 60 mg/L nitrate plumed reduces the barrier longevity to about 7 to 10 years. However, less than three years after sodium dithionite injection, chromium concentrations in some of the wells increased (Figure 2), indicating that the treated aquifer has been losing its reductive capacity. In 2002, some barrier wells were re-injected with sodium dithionite to re-establish reductive capacity in the aquifer at these locations. Since then, however, chromium has been detected in several more wells, again indicating premature loss of reductive capacity in the aquifer. The original prediction of barrier longevity was based on average values of the quantity and distribution of Fe(II), flow rates through each discrete interval of the treatment zone, and concentrations of oxidizing constituents in the incoming groundwater, assuming a relatively homogeneous aquifer. In the original computations, the oxidizing effects of the nitrate plume were not incorporated. However, while the presence of nitrate reduces barrier longevity uniformly, it does not account for the specific breakthrough locations (Szecsody et al. 2005). Possible causes for premature chromate breakthrough are associated with the presence of high-permeability zones in the aquifer (DOE 2004a, b). In these zones, groundwater moves relatively fast and is able to oxidize Fe(II) more rapidly. In addition, given the physical and chemical heterogeneity of the aquifer, it is possible that the high-permeability flow paths may be deficient in reducing equivalents (e.g., reactive iron), which is required for dithionite treatment performance.

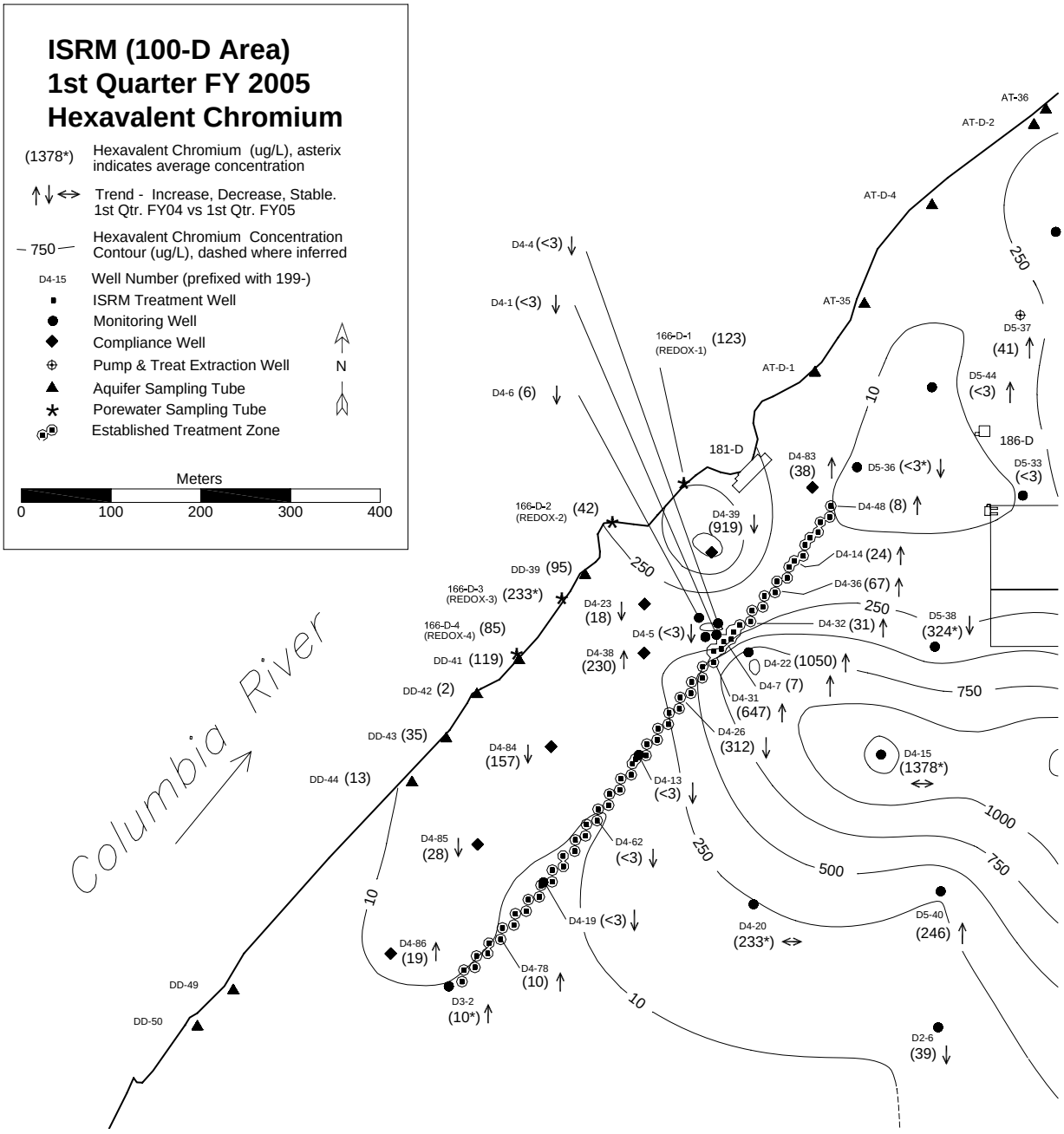

Figure 1. Hanford Site 100-D ISRM Barrier Location and Chromate Plume (FHI 2005)

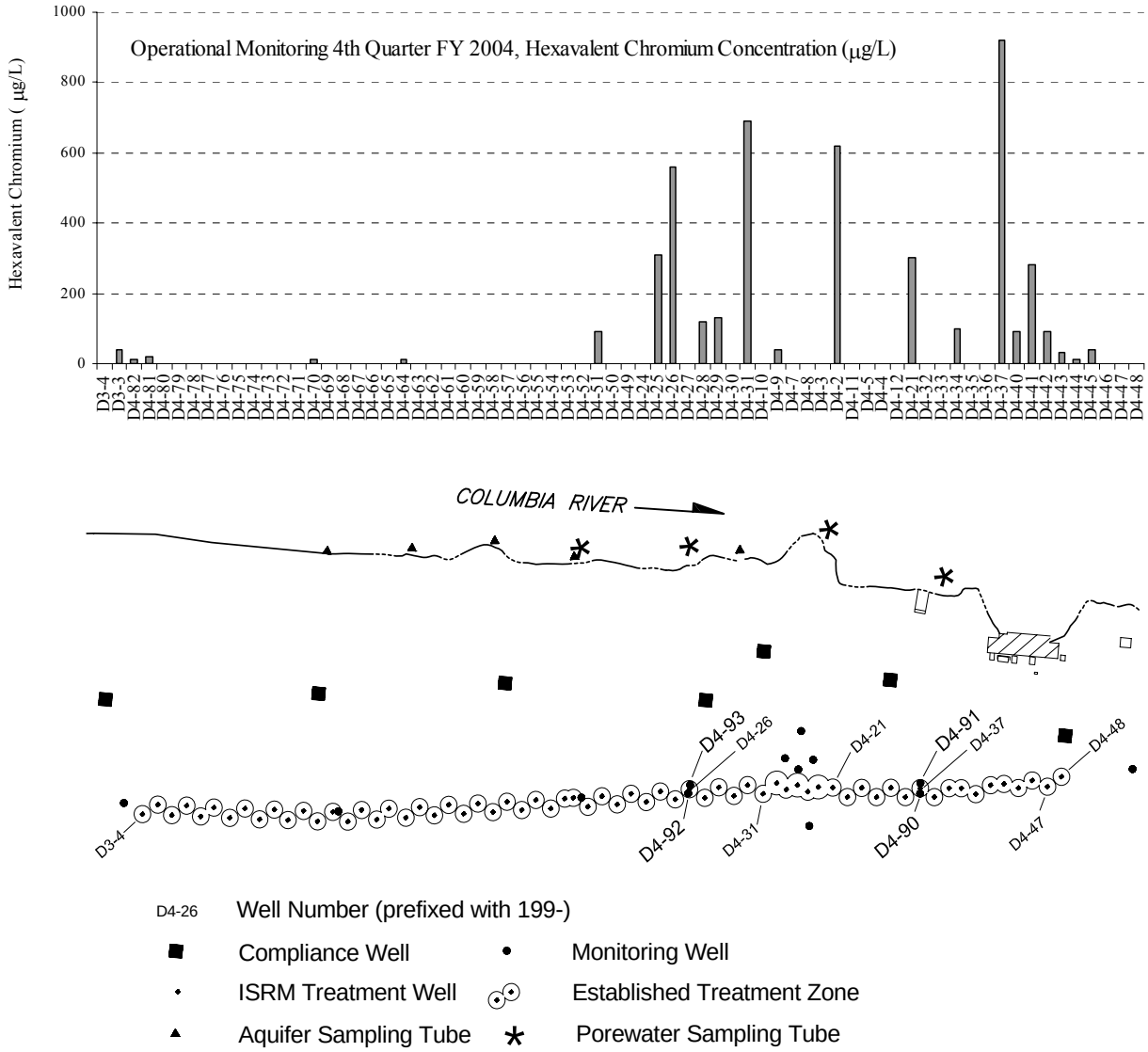

Figure 2. 100-D ISRM Well Chromate Concentrations (12/2004) and Borehole Locations Where Sediment Was Obtained for This Study (D4-90, D4-91, D4-92, D4-93). Boreholes are 10 to 12 ft up- and downgradient of D4-26 and D4-37 (DOE-2005)

One way enhancement of the current barrier reductive capacity can be achieved is by the addition of micron-scale zero-valent iron. This type of iron has been evaluated as a material to remediate a wide range of groundwater contaminants (Gillham and O'Hannisin 1994) because of it is an extremely strong chemical reductant. A particularly attractive feature of zero-valent iron is the potential to produce three electrons for Cr(VI) reduction compared to just one electron for Fe(II) reduction. Kaplan et al. (1994, 1996) showed the potential of injecting colloidal size Fe^0 (1–3 micron diameter) as a suspension into porous media. Due to the high density of the Fe^0 particles (7.6 g/cm^3), it was rather difficult to force these particles a considerable distance into porous media at significant concentrations. Flow rates much greater than typical groundwater were required to move the Fe^0 colloids through the sand columns. The primary removal

mechanism of the iron colloids in the aqueous solutions was assumed to be gravitational settling (Kaplan et al. 1994, 1996). Cantrell et al. (1997a, b) conducted column studies with several shear-thinning fluids to enhance Fe^0 colloid emplacement. The viscosity of these fluids decreases with increasing shear rate, resulting in a relatively high solution viscosity near the iron particles where the shear stress is low, relative to locations near the surfaces of porous media, where the shear stress is relatively high. The primary reason to use these additives was to create a suspension that is viscous enough to keep the Fe^0 in suspension for extended time periods to improve colloid mobilization into the porous media, while not causing a detrimental decrease in hydraulic conductivity.

Polymer flooding has been used in various subsurface applications. Injection of polymer solutions has been an established enhanced oil recovery (EOR) method to improve oil production over standard water flooding (Lake 1989). Martel et al. (1998) used the technique to obtain mobility control for displacement in heterogeneous, layered porous media in flow cells. They showed that injecting the polymer xanthan resulted in increased sweep efficiency through improved access to lower-permeability materials and eliminated viscous fingering at the polymer displacement front. Based on their experimental results, they argued that polymer/surfactant combinations could be used for NAPL removal from lower permeability layers. Kostarelos et al. (1998) used the polymer xanthan in a flushing solution containing surfactant and alcohol used to remove liquid trichloroethylene (PCE) from a flow cell. The polymer was added to stabilize dense micro-emulsions containing the PCE.

Some iron emplacement will occur due to interception onto the porous medium matrix surfaces. As the velocity of the injected polymer solution decreases with its radial distance from the injection well, gravitational settling of the particles from the solution becomes increasingly important. Cantrell et al. (1997a, b) used three nontoxic polymers at different concentrations in 1-m-long columns containing laboratory sands. They showed that the use of shear-thinning fluids greatly improved the injectability and mobility of the iron suspensions in porous media. They clearly demonstrated that the polymer Slurry Pro CDP (K.B. Technologies, Chattanooga, TN) performed best overall, producing iron enhancement of up to 1% (w/w) when 30 pore volumes of a 1% iron solution were injected. In a larger column (3 m), the iron concentrations ranged from 0.27 at the inlet to 0.1% near the outlet. The experimental results showed that effective addition of the polymers could be obtained at much lower velocities than those needed to inject iron into porous media without added polymers (Kaplan et al. 1994, 1996). Later work by the same authors, focusing on the injection of these suspensions into Hanford Site sediments, showed results that were quite promising: no adsorption of the polymer material on the aquifer materials and a fairly even distribution of iron throughout meter-long columns (DOE 2004a).

Previous iron emplacement studies with polymer additions have only been conducted with homogeneous porous media in one-dimensional columns. Detailed experiments in heterogeneous systems using multidimensional flow cells have not been performed. The objective of this study was, therefore, to investigate in a three-dimensional wedge-shaped flow cell the potential emplacement of zero-valent iron into high-permeable Hanford Site sediments (Ringold Unit E

gravels) using shear-thinning fluids containing polymers. As a minimum, the emplaced iron should provide at least the average reductive capacity currently provided by Fe(II) iron, estimated to be approximately 11.0 ± 3 μmol Fe(II)/g of sediment (Szecsody et al. 2005). Because zero-valent iron is potentially able to provide three times more electrons than Fe(II), an amendment of at least 5-μmol zero-valent iron/g of sediment would be considered a satisfactory result. Expressed in weight percent, this minimum amended concentration equals approximately 0.03%. The experiments were conducted in an intermediate-scale, wedge-shaped flow cell to mimic radial flow conditions. Porous media were packed in the flow cell to create either a heterogeneous layered system with a high-permeability zone between two low-permeability zones or a high-permeability channel surrounded by low-permeability materials. The injection flow rate, polymer type, polymer concentration, and injected pore volumes were determined based on preliminary short- and long-column experiments.

2.0 Materials and Methods

The laboratory experiments consisted of Fe^0 emplacement studies in water saturated 20-cm-long columns, 1-m-long columns, and an intermediate-scale wedge-shaped flow cell. The primary purpose of the column experiments was to determine the most promising treatment to be used in the intermediate-scale flow cell. The short, 20-cm column was used for preliminary displacement tests using two porous media, two zero-valent iron types, two polymer types, two polymer concentrations, three pore-volumes, and three different injection velocities, for a total of 44 experiments. The experimental details for the short columns are listed in Table 1. Due to the limited availability of Ringold E sediment, 32 experiments were conducted with 12/20 Accusand (Unimin Corporation, Le Sueur, MN). From these experiments, eight treatments were repeated in the short columns using the permeable Ringold E sediment. Of these eight treatments applied to the Ringold E sediment, the two best treatments were used in 1-m-long columns for both porous media types. Results from these experiments were then used to select one treatment for investigation using the wedge-shaped flow cell. The performance criteria used were magnitude and uniformity of the amended zero-valent concentration in the columns.

Table 1. Overview of 20-cm Column Experiments. Prefixes A and R in experiment name denote 12/20 Accusand and Ringold E sediment, respectively.

Experiment number	Flow rate (cm/s)	Pore volume	Polymer	Polymer conc. (% w/w)
A-1	0.01	3	SP	0.01
A-2	0.01	3	SP	0.02
A-3	0.01	3	AMPS	0.25
A-4	0.01	3	AMPS	0.50
A-5	0.01	10	SP	0.01
A-6	0.01	10	SP	0.02
A-7	0.01	10	AMPS	0.25
A-8	0.01	10	AMPS	0.50
A-9	0.01	30	SP	0.01
A-10	0.01	30	SP	0.02
A-11	0.01	30	AMPS	0.25
A-12	0.01	30	AMPS	0.50
A-13	0.02	3	SP	0.01
A-14	0.02	3	SP	0.02
A-15	0.02	3	AMPS	0.25
A-16	0.02	3	AMPS	0.50
A-17	0.02	10	SP	0.01
A-18	0.02	10	SP	0.02
A-19	0.02	10	AMPS	0.25
A-20	0.02	10	AMPS	0.50
A-21	0.02	30	SP	0.01

Table 1 (Contd)

Experiment number	Flow rate (cm/s)	Pore volume	Polymer	Polymer conc. (% w/w)
A-22	0.02	30	SP	0.02
A-23	0.02	30	AMPS	0.25
A-24	0.02	30	AMPS	0.50
A-25	0.05	3	SP	0.01
A-26	0.05	3	SP	0.02
A-27	0.05	3	AMPS	0.25
A-28	0.05	3	AMPS	0.50
A-29	0.05	10	SP	0.01
A-30	0.05	10	SP	0.02
A-31	0.05	10	AMPS	0.25
A-32	0.05	10	AMPS	0.50
A-33	0.05	30	SP	0.01
A-34	0.05	30	SP	0.02
A-35	0.05	30	AMPS	0.25
A-36	0.05	30	AMPS	0.50
R-1	0.02	10	SP	0.01
R-2	0.02	10	SP	0.02
R-3	0.02	10	AMPS	0.25
R-4	0.02	10	AMPS	0.50
R-5	0.02	30	SP	0.01
R-6	0.02	30	SP	0.02
R-7	0.02	30	AMPS	0.25
R-8	0.02	30	AMPS	0.50

2.1 Porous Media

The high permeability Ringold Unit E sediments used in this study were obtained from four borehole, D4-90, D4-91, D4-92, and D4-93, drilled within the ISRM barrier (Figure 2). For this study, Ringold sediments with diameters between 0.1 and 1.0 cm were obtained from the available borehole materials and thoroughly mixed. The saturated hydraulic conductivity, obtained using a constant head method (Klute and Dirksen 1986) for five different packings, was 0.42 ± 0.12 cm/s or approximately 20 times the average aquifer hydraulic conductivity estimate obtained from a multiple well constant rate discharge test at the site (Williams et al. 2000). Because only a limited amount of Ringold sediment was available to be used for these experiments, the initial series of 20-cm column experiments was conducted with 12/20 Accusand (Unimin Corporation, La Sueur, MN). This laboratory sand has a hydraulic conductivity of 0.5 cm/s (Schroth et al. 1996), which is comparable to hydraulic conductivity value of high-permeability Ringold porous media (Szecsody et al. 2005).

2.2 Zero-valent Iron Types

The two micrometer-scale iron particles used in the experiments were S-3700 Fe^0 colloids with a diameter of 2 ± 1 μm (International Specialty Products, Wayne, NJ) and H-200 Special Zerovalent Iron with a diameter of 43 ± 5 μm (ARS Technologies, New Brunswick, NJ). The S-3700 particles have been tested extensively in both batch and column experiments (Cantrell et al. 1997a, b; Cantrell and Kaplan 1997; Kaplan et al. 1994), while the H-200 iron has been successfully used to construct reactive barriers at many sites. All experiments were conducted with 1% (w/w) iron concentration colloid suspension, and each colloid suspension contained 0.001% aerosol (Sigma Chemical, St. Louis, MO). The Fe^0 particles were dispersed in the surfactant solution before the polymer was added.

2.3 Polymers

Two polymer compounds were used for testing the efficacy of non-Newtonian fluids to enhance the displacement of zero-valent iron colloid suspensions. Based on the column experiments by Cantrell et al. (1997a, b), the synthetic high-molecular weight polymer Slurry Pro CDP (K.B. Technology, Chattanooga, TN) was selected. The second polymer was sodium-2-acrylamido-2-methylpropane sulfonate (Sigma Chemical Co.) based on successful displacement experiments with Hanford Site porous media (DOE 2004a, Appendix E). In this report, the Slurry Pro and sulfonate polymers are denoted as SP and AMPS, respectively. Based on polymer-enhanced iron displacement experiments by Cantrell et al. (1997a, b), the selected SP concentrations were 0.01 and 0.02 % w/w. The used AMPS concentrations were 0.25 and 0.5% w/w, based on previous experimental work discussed in DOE (2004a).

2.4 Column Experiments

The 20-cm acrylic column had a diameter of 10 cm and consisted of two stackable 10-cm sections. The iron suspensions were injected using a Masterflex laboratory pump. The inlet end of the columns was equipped with a cone-shaped tapered reducer to provide an even distribution across the cross-sectional area of the column. The 1-m-long column was similar to the smaller column except that ten stackable 10-cm compartments were used. After each experiment, the contents in each section were mixed and three 20-g samples obtained for the iron analyses. To be consistent with the iron enhancement studies by Kaplan et al. (1996) and Cantrell et al. (1997a, b), the number of pore volumes injected into the columns was 3, 10, and 30. The flow rates used in the 20-cm column studies were 0.01, 0.02, and 0.05 cm/s. Cantrell et al. (1997a, b) found that flow rates larger than 0.05 cm/s resulted in insufficient gravitational settling and relatively low iron concentrations throughout the entire 1-m-long columns.

2.5 Flow Cell Experiments

The wedge-shaped flow cell (Figure 3) was made out of ⅜-inch polyethylene with a ¾-inch acrylic lid. Figure 4 is a top view of the flow cell with the horizontal dimensions and sample locations. The flow cell, representing an 18^{o} wedge, is 20 cm deep. The total volume of the flow cell is 59 L (15.6 gal). The porous media were packed into the flow cell to create either a high-permeability channel surrounded by low-permeability materials (Experiment 1) or a heterogeneous layered system with a high-permeability zone between two low-permeability zones (Experiment 2). The configuration of the first experiment represents a high-permeability channel surrounded by low permeability material. The cross-sectional views of the outflow end of Experiment 1 and 2 are shown in Figures 5 and 6, respectively. Figure 5 presents a plan view of the channel location in Experiment 1. The low-permeability material used in the two flow cell experiments was 70-mesh Accusand. The saturated hydraulic conductivity of this material was determined to be 7.8×10^{-3} cm/s, which is almost 2 orders of magnitude less than the highly permeable Ringold material. The channel volume in Experiment 1 was 21.9 L (5.8 gal). A total of 42.7 kg of Ringold material was packed in this zone, resulting in a dry bulk density of 1950 kg/m^3 and a porosity of 0.264. The Ringold layer in Experiment 2 had a volume of 29 L (7.7 gal) and a total of 57.8 kg Ringold material was used, resulting in an average dry bulk density of 1993 kg/m^3 and a porosity of 0.248. The porosity calculations were based on a particle density of 2650 kg/m^3.

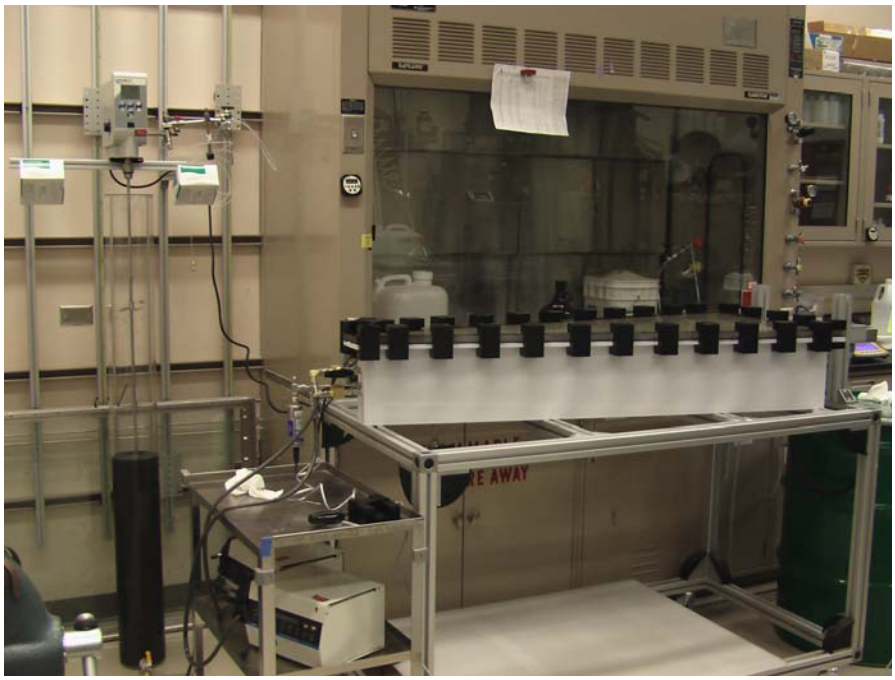

Figure 3. Experimental Setup of Flow Cell Experiment. The iron suspension is mixed in a 20-L cylindrical container before it is pumped into the flow cell using two Masterflex laboratory pumps. The outflow boundary is controlled using a constant-head chamber. Iron suspension leaving the flow cell is collected in 55-gal waste drums.

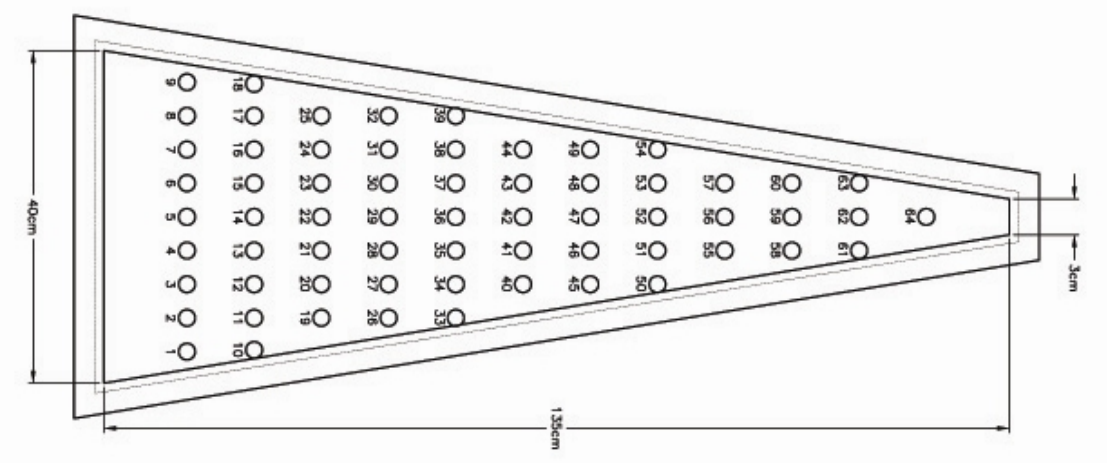

Figure 4. Sampling Locations for Each of the Five Levels in the Flow Cell

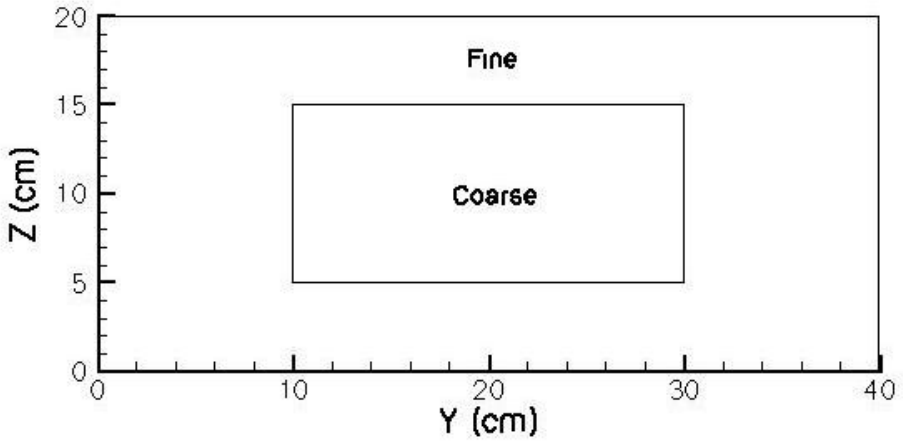

Figure 5. Cross-Sectional View of the Outflow End of Flow Cell Experiment 1. A Ringold high-permeability channel is surrounded by fine-grained 70-Accusand.

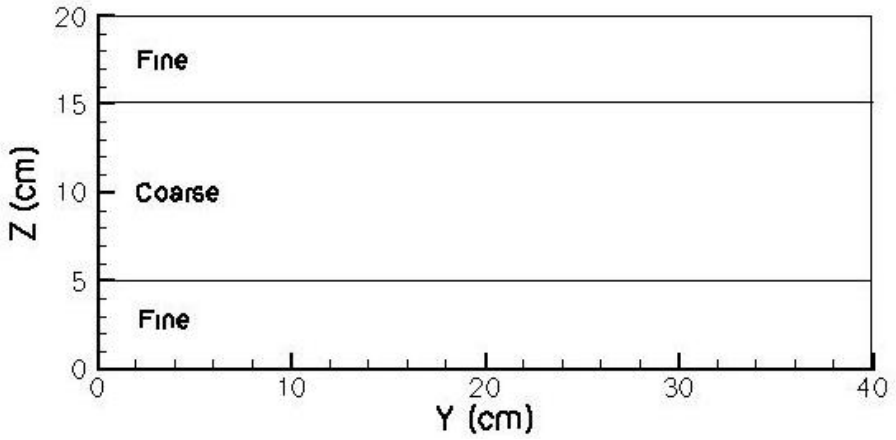

Figure 6. Cross-Sectional View of the Outflow End of Flow Cell Experiment 2. A Ringold high-permeability layer is located between fine-grained 70-Accusand layers.

Both experiments were sampled at five levels. The level locations are at 2.5 cm (Level 1), 7.5 cm (Level 2), 10 cm (Level 3), 12.5 cm (Level 4), and 17.5 cm (Level 5) from the bottom. Sixty-four samples were taken at each level. The sampling locations of each level are shown in Figure 7. Samples were taken with 4-cm-long, 1-cm inside-diameter aluminum pipe samplers. First, the porous medium was first excavated to 0.5 inch above each level. The samplers were then inserted 1 inch into the porous medium and excess porous material around each sampler was removed. The sampler insertion was repeated for each layer for a total of 5 × 64 = 320 samples per experiment. A 50-mL vial was then placed upside down over the sampler and a 1/32-inch-thick aluminum plate was placed underneath the sampler to prevent loss of material. The vial-sampler-aluminum plate combination was carefully lifted and turned so that the porous material was deposited in the vial. The samples were oven-dried and weighted.

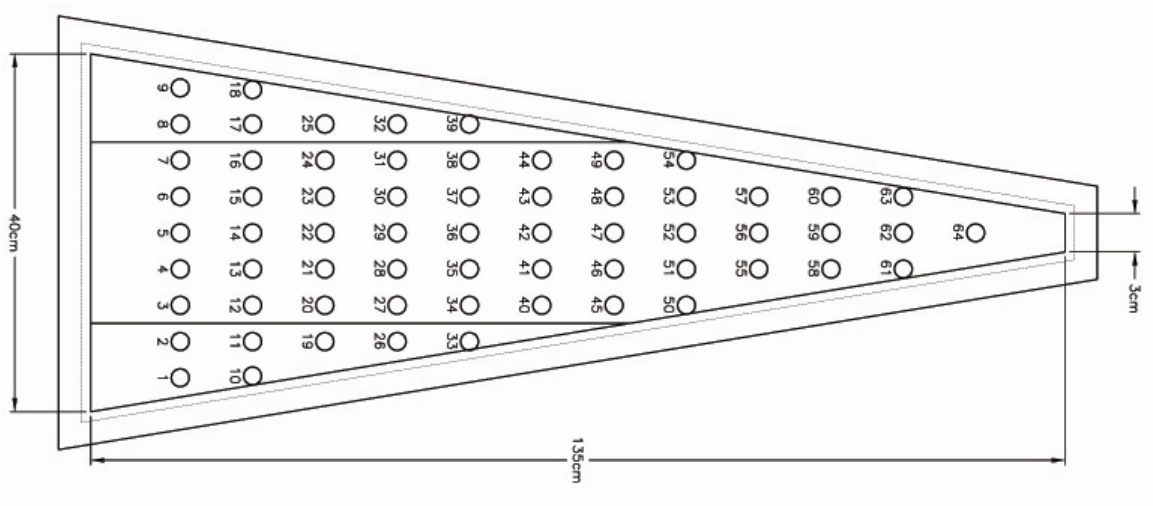

Figure 7. Plan View of Flow Cell Experiment 1 with the Location of the High-Permeability Channel

2.6 Sample Analysis

The porous media samples from the columns and flow cell were analyzed for iron using an inductively coupled plasma mass spectrometer (ICP-MS) after treatment with HCl (5 M) for two weeks to dissolve the iron. All reported Fe^0 concentrations are in % w/w and were corrected for native iron oxide content of the porous media. The iron oxide concentrations of 12/20 Accusand, 70-Accusand, and high-permeability Ringold porous media were 0.04 ± 0.003, 0.02 ± 0.002, and 0.84 ± 0.06 % (w/w), respectively. The values represent the average of 20 samples per porous medium. The values for the two Accusands are consistent with the analytical results reported by Schroth et al. (1996), while the native iron concentration corresponds well to the average value obtained by Szecsody et al. (2005) for 68 samples from the four boreholes. Not all of this native iron is available for oxidation. Szecsody et al. (2005) demonstrated that approximately 10% of this iron contributes to the field reductive capacity.

3.0 Results and Discussion

3.1 Short-Column Experiments with 12/20 Accusand

Unfortunately, the injections with H-200 iron yielded unfavorable results. The polymer solutions were unable to carry the iron particles homogeneously through the 20-cm columns. Right after entering the column, the H-200 particles settled to the bottom. This tendency is shown in Figure 8a for a 0.02% Slurry Pro treatment with a flow rate of 0.05 cm. Figures 8b and 8c show the top and bottom of the column after injection of 30 pore volumes. Figure 8b shows that the top has not been contacted by iron, but the bottom is very dark, indicating heavy iron precipitation. This iron type could not be transported uniformly because of the relatively large size of the particles (43 ± 5 μm). Because the iron was displaced nonuniformly in the columns for both polymers at the highest concentration, H-200 was removed from consideration. Samples from the H-200 experiments were not analyzed because of the nonuniform distribution.

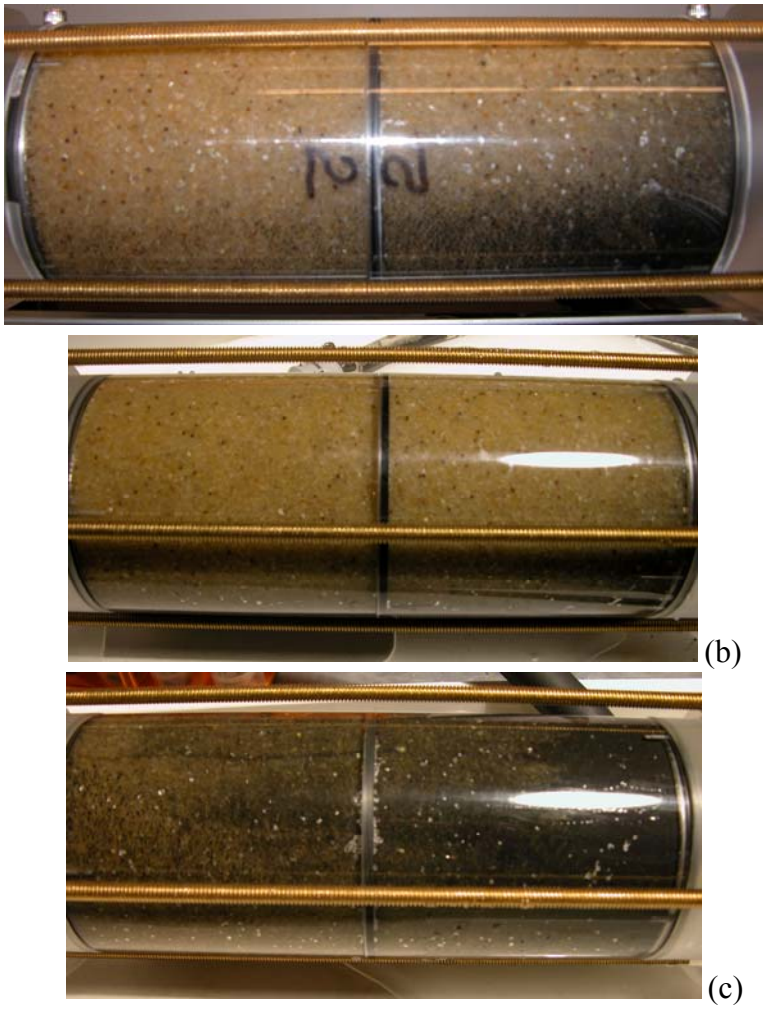

(a) (b) (c)

Figure 8. H-200 Iron Suspension Injection at 0.05 cm/s with 0.02% SP after 30 Pore Volumes: (a) side, (b) top, and (c) bottom views

The 20-cm-column experiments with the S-3700 iron did not show the density effects observed for the H-200 iron. In all experiments, the iron particles appeared to move through the column uniformly. An example is shown in Figure 9 for injection of S-3700 in 12/20 Accusand using a 0.02% SP suspension at 0.02 cm/s. The suspension moves in as a vertical front and, as indicated by the pictures, the column becomes darker indicating increasing deposited iron levels.

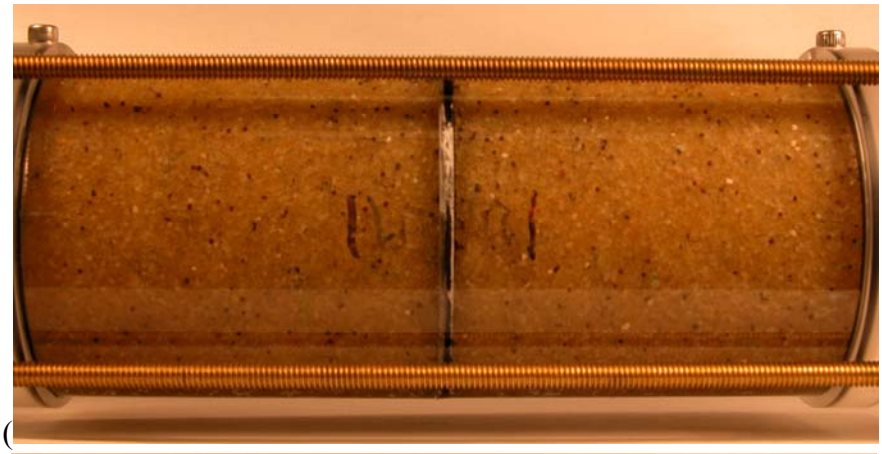

(a)

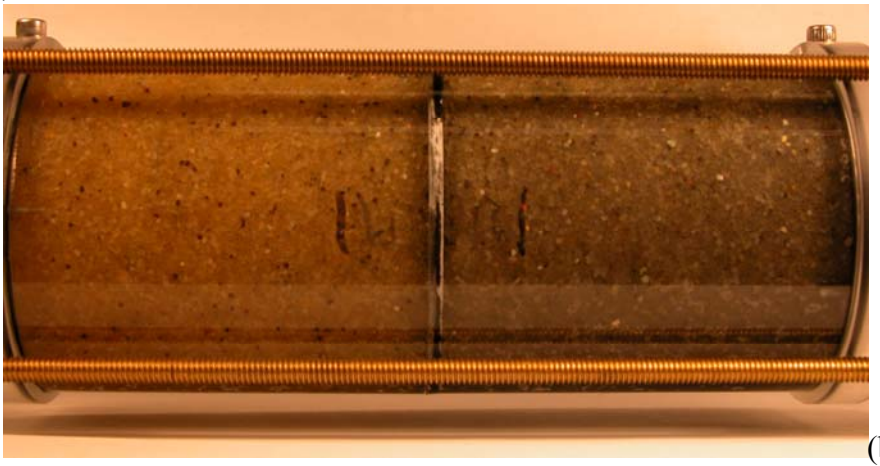

(b)

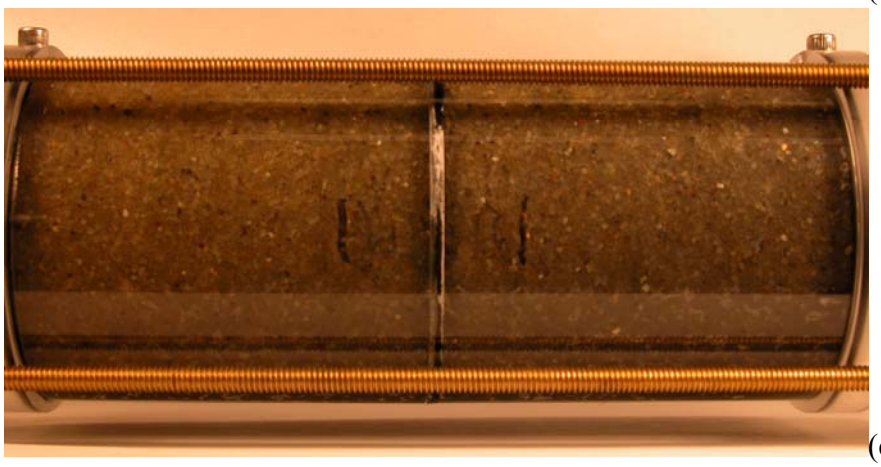

(c)

Figure 9a. Injection of S-3700 in 12/20 Accusand Using a 0.02% SP Suspension at 0.02 cm/s after (a) 0, (b) 0.5, and (c) 1 Pore Volume

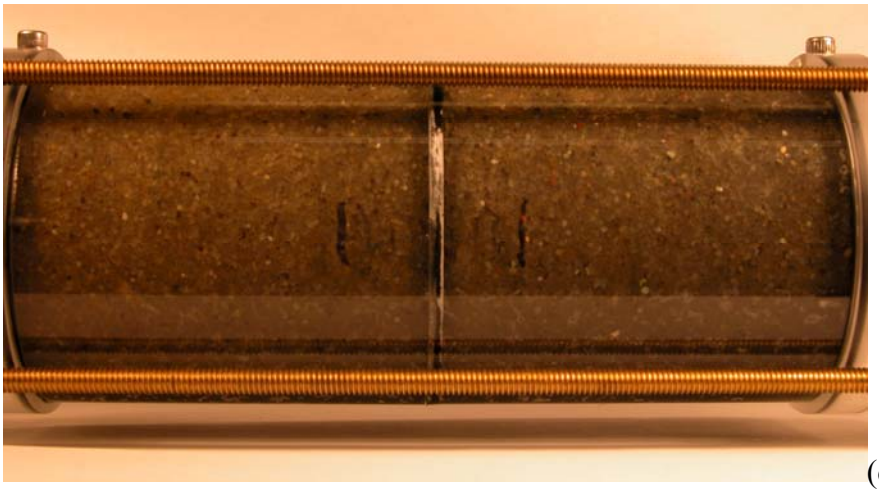

(d)

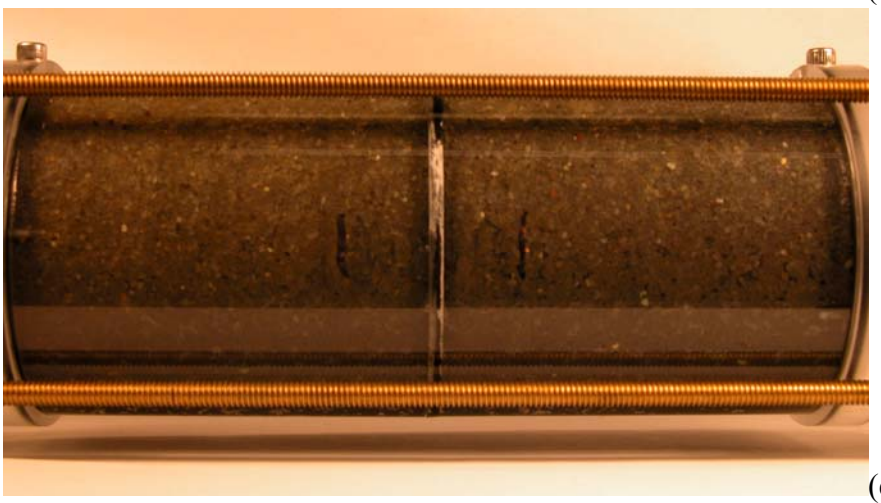

(e)

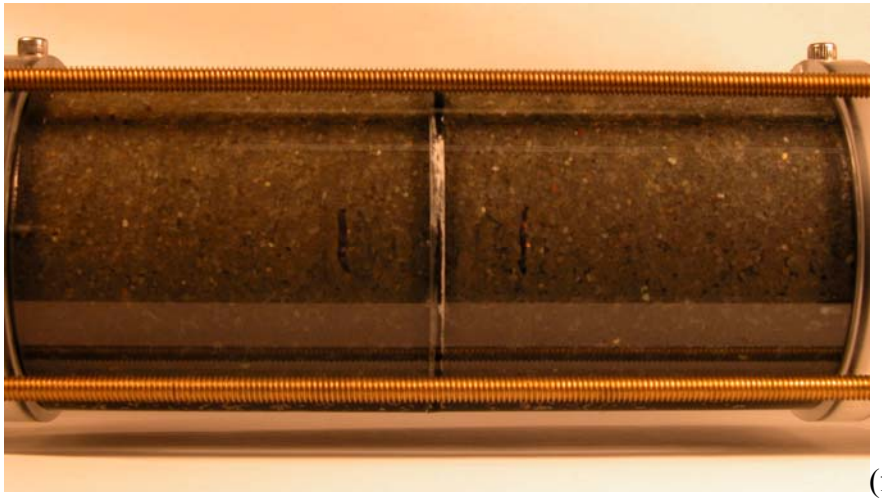

(f)

Figure 9b. Injection of S-3700 in 12/20 Accusand Using a 0.02% SP Suspension at 0.02 cm/s after (d) 3, (e) 10, and (f) 30 Pore Volumes

The iron concentrations for the S-3700 treatments in 12/20 Accusand are listed in Table 2. The results show the emplaced iron concentrations are always higher in the first section and the concentrations generally increase with an increase in injected pore volumes. The highest

concentrations were obtained for cases receiving the largest number of pore volumes of treatment. The 0.02 cm/s flow rate produced generally higher amended iron concentrations in the second section than the 0.01 and 0.05 cm/s applications. The slowest flow rate applications show large differences between the first and second section. The highest flow rate resulted in smaller concentrations in both compartments compared to the 0.02 cm/s. The results in Table 2 show no obvious differences between the polymer types, although the highest polymer concentration applications appear to deposit more iron. Based on the results listed in Table 2, it was decided to complete the 20-cm columns experiments without considering the 3 pore volume, the 0.01 cm/s and 0.05 cm/s applications. The remaining eight treatments are listed in Table 3.

Table 2. Amended Fe^0 Concentrations (% w/w) for 20-cm Column Experiments with 12/20 Accusand and S-3700 Iron

Experiment number	Flow rate (cm/s)	Pore volume	Polymer	Polymer conc. (% w/w)	Fe^0 (% w/w) 1st section	Fe^0 (% w/w) 2nd section
1	0.01	3	SP	0.01	0.32	0.07
2	0.01	3	SP	0.02	0.41	0.11
3	0.01	3	AMPS	0.25	0.29	0.12
4	0.01	3	AMPS	0.50	0.26	0.15
5	0.01	10	SP	0.01	1.01	0.32
6	0.01	10	SP	0.02	0.93	0.35
7	0.01	10	AMPS	0.25	1.11	0.24
8	0.01	10	AMPS	0.50	0.97	0.32
9	0.01	30	SP	0.01	1.72	0.67
10	0.01	30	SP	0.02	1.61	0.89
11	0.01	30	AMPS	0.25	1.56	0.73
12	0.01	30	AMPS	0.50	1.44	0.76
13	0.02	3	SP	0.01	0.37	0.17
14	0.02	3	SP	0.02	0.46	0.17
15	0.02	3	AMPS	0.25	0.39	0.15
16	0.02	3	AMPS	0.50	0.40	0.19
17	0.02	10	SP	0.01	1.24	0.65
18	0.02	10	SP	0.02	1.09	0.78
19	0.02	10	AMPS	0.25	1.19	0.52
20	0.02	10	AMPS	0.50	1.07	0.61
21	0.02	30	SP	0.01	1.67	1.22
22	0.02	30	SP	0.02	1.45	1.43
23	0.02	30	AMPS	0.25	1.39	1.29
24	0.02	30	AMPS	0.50	1.27	1.07
25	0.05	3	SP	0.01	0.23	0.15
26	0.05	3	SP	0.02	0.27	0.22
27	0.05	3	AMPS	0.25	0.20	0.25

Table 2 (Contd)

Experiment number	Flow rate (cm/s)	Pore volume	Polymer	Polymer conc. (% w/w)	Fe^0 (% w/w) 1st section	Fe^0 (% w/w) 2nd section
28	0.05	3	AMPS	0.50	0.19	0.13
29	0.05	10	SP	0.01	1.03	0.45
30	0.05	10	SP	0.02	0.87	0.56
31	0.05	10	AMPS	0.25	0.99	0.50
32	0.05	10	AMPS	0.50	1.01	0.41
33	0.05	30	SP	0.01	1.21	0.78
34	0.05	30	SP	0.02	1.04	1.02
35	0.05	30	AMPS	0.25	1.19	0.87
36	0.05	30	AMPS	0.50	1.06	0.91

Table 3. Amended Fe^0 Concentrations (% w/w) for 20-cm Column Experiments with Ringold E Sediment and S-3700 Iron

Experiment number	Flow rate (cm/s)	Pore volume	Polymer	Polymer conc. (% w/w)	Fe^0 (% w/w) 1st section	Fe^0 (% w/w) 2nd section
R-1	0.02	10	SP	0.01	0.87	0.47
R-2	0.02	10	SP	0.02	0.79	0.54
R-3	0.02	10	AMPS	0.25	1.12	0.39
R-4	0.02	10	AMPS	0.50	0.89	0.56
R-5	0.02	30	SP	0.01	1.21	0.85
R-6	0.02	30	SP	0.02	1.33	1.17
R-7	0.02	30	AMPS	0.25	1.11	0.64
R-8	0.02	30	AMPS	0.50	1.16	1.22

3.2 Short-Column Experiments with Ringold-E Sediment

An example of a polymer injection in the Ringold sediment is shown in Figure 10 for 0.02% Slurry Pro suspension with an injection rate of 0.02 cm/s. The suspension displacement was stable with a vertical front. Over time the column is darkened, indicating increased iron precipitation. The results in Table 2 show that the 30 pore volume injection resulted in higher amended iron concentrations. No clear differences between the two polymers were observed although the highest polymer concentrations yielded larger iron concentrations in the second compartment. Based on these results, it was decided to use the 0.02 cm/s, 30 pore volume application for both polymers at the highest concentration in the 1-m-long columns.


(a)


(b)


(c)


(d)

Figure 10a. Injection of S-3700 in High-Permeability Ringold Material Using a 0.02% SP Suspension at 0.02 cm/s after (a) 0, (b) 0.5,(c) 1, and (d) 3 Pore Volumes

(e)

Figure 10b. Injection of S-3700 in High-Permeability Ringold Material Using a 0.02% SP Suspension at 0.02 cm/s after 10 Pore Volumes

3.3 Long-Column Experiments

The results of the four 1-m-long column studies are shown in Figure 11, where the amended percent zero-valent iron is plotted versus distance from the column inlet. The results show a larger decline in iron concentrations for the AMPS applications, relative to the SP treatment, for both the 12/20 as the Ringold sediment. The SP applications also show a decline in the first 40 cm, but the iron concentrations for both porous media leveled off in the downstream half of the column. The iron concentrations for the Ringold material settled at a value slightly above 0.6% (w/w). The results of the 1-m-long column application show that the SP polymer suspensions provided better results than the AMPS applications. The combined results of the

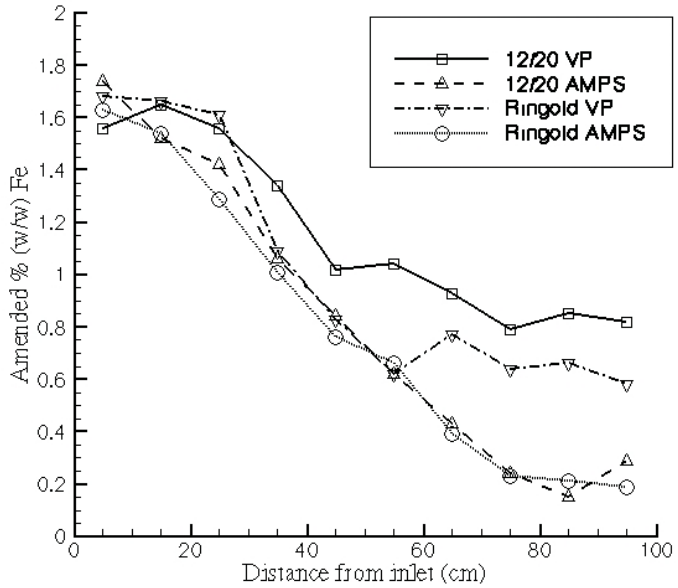

Figure 11. Amended % (w/w) Fe^0 as Function of Distance from Inlet for SP and AMPS Treatments Using 12/20 Accusand and Ringold Sediment after 30 Pore Volumes

short and long column experiments indicated that the 30-pore volume application at a 0.02 cm/s flow rate with the 0.02% SP polymer would provide the best chance of a successful application in the intermediate-scale wedge-shaped flow cell.

3.4 Flow Cell Experiments

Based on the column experiment results, 30 pore volumes of 0.02% SP at 0.02 cm/s were injected for the flow cell experiments. The flow rate was assumed to apply to the outflow end of the flow cell. The injection rate for Experiment 1, with a 200 cm^2 zone of highly permeable Ringold, was 240 mL/min. In Experiment 2, with a 400 cm^2 zone of high-permeability Ringold, the injection rate was 480 mL/min. The duration of Experiment 1, with an estimated pore volume of 5.8 L, was 12 hours. Experiment 2, with a pore volume of 7.7 L, lasted 8 hours. The injection rates were ramped up linearly to the intended rate over 15 minutes to avoid excessive initial pressures in the system. This ramping method was determined necessary after an initial flow experiment showed that the upper low-permeability material fractured when the flow rate was immediately set to the maximum of 480 mL/min. The fractures resulted in preferential flow of the injected iron along the top of the flow cell (Figure 12).

Figure 13 shows the excavated surfaces for sampling Levels 2, 3 and 4 for Experiment 1. The pictures show the intense dark color of the Ringold sediment throughout the flow cell, indicating that iron has precipitated fairly homogeneously. The pictures also show that the surrounding 70-Accusand transported only minor amounts of iron. Figure 14 is a picture of the inserted samplers for Level 2, where visual observation of the excavated levels showed similar results. Based on the dark colors, iron was deposited throughout the flow cell at Levels 2, 3, and 4. Figure 15 provides an overview of the excavated surface for sampling at Level 2. Fluid pressure measurements near the injection location show that in Experiment 1 the pressure slowly increased to ~20 KPa (~3 psi) and in Experiment 2 to ~25 KPa (~3.5 psi) above background pressure. These elevated pressures appear to be related to the increased viscosity of the polymer solutions. No obvious negative effects of reduced saturated hydraulic conductivity were observed in either experiment.

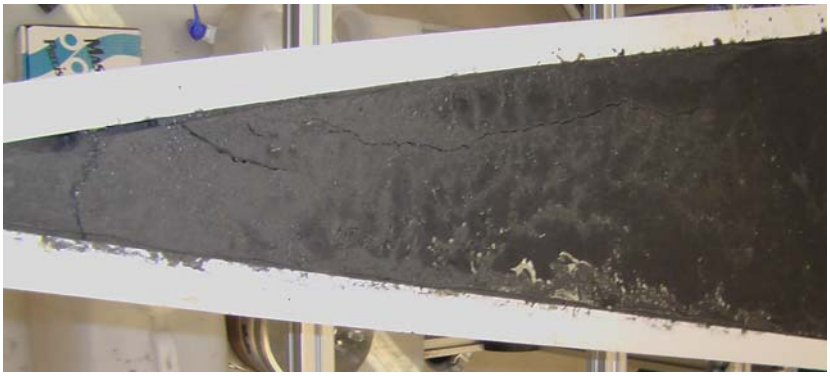

Figure 12. Top View of Failed Flow Cell Experiment Due to Fracturing of Upper Low-Permeability Layer when Iron Injected at 480 mL/min

(a)

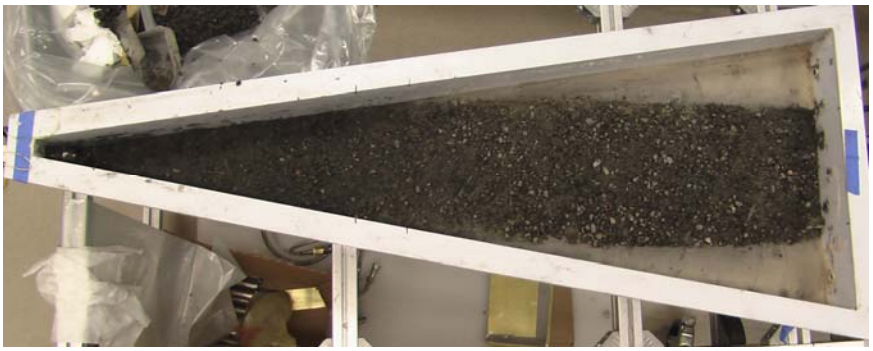

(b)

(c)

Figure 13. Excavated Surfaces for Sampling in (a) Level 2 (12.5 cm from bottom), (b) Level 3 (10 cm from bottom) and (c) Level 4 (7.5 cm from bottom) for Experiment 1

Figure 14. Excavated Surface for Level 2 with Inserted Samplers for Experiment 1

Iron distributions as a function of distance from the inlet are shown in Figure 16 for Experiment 1 and Figure 17 for Experiment 2. The iron concentrations for all the sampling locations of both experiments are listed in the appendix at the end of this report. Both plots show that the differences in iron content for the various Ringold levels (Level 2, 3, and 4) are minor, indicating that the iron has been transported relatively uniformly as a function of elevation. Another observation is that only small amounts of iron have moved into the lower permeability zones (Level 1 and 2). Although the iron concentrations generally decrease as a function of distance from the injection location, the iron concentrations at the downstream half of the flow cell seem to level out at concentrations of about 0.6% in both experiments.

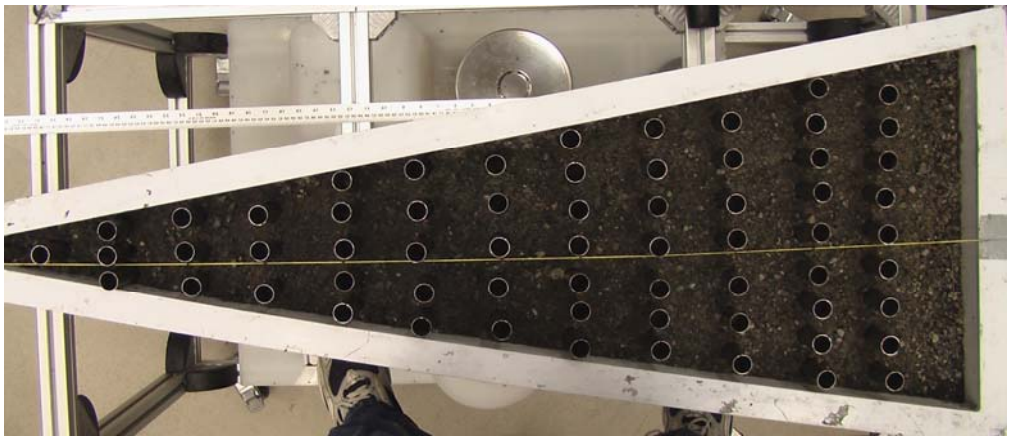

Figure 15. Excavated Surface for Level 2 with Inserted Samplers for Experiment 2

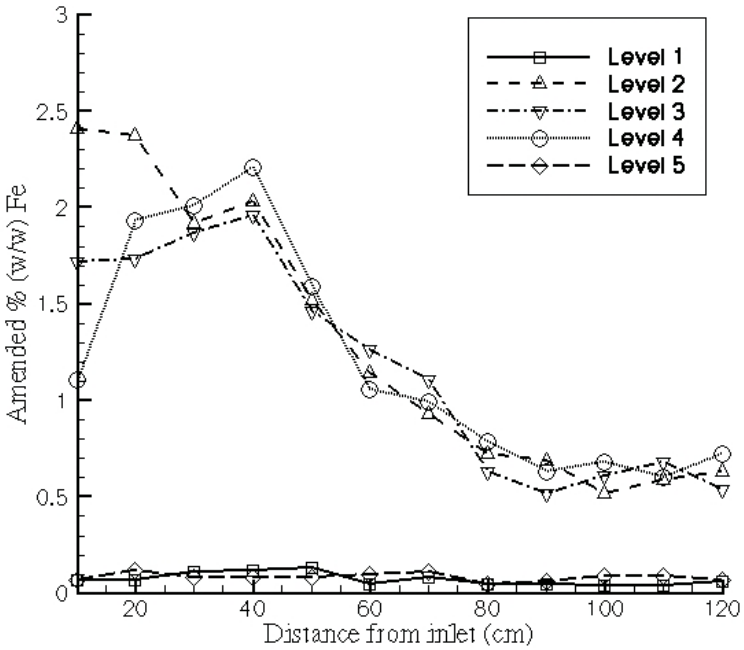

Figure 16. Amended % (w/w) Fe^0 at all Five Levels as a Function of Distance from Injection Location (Experiment 1)

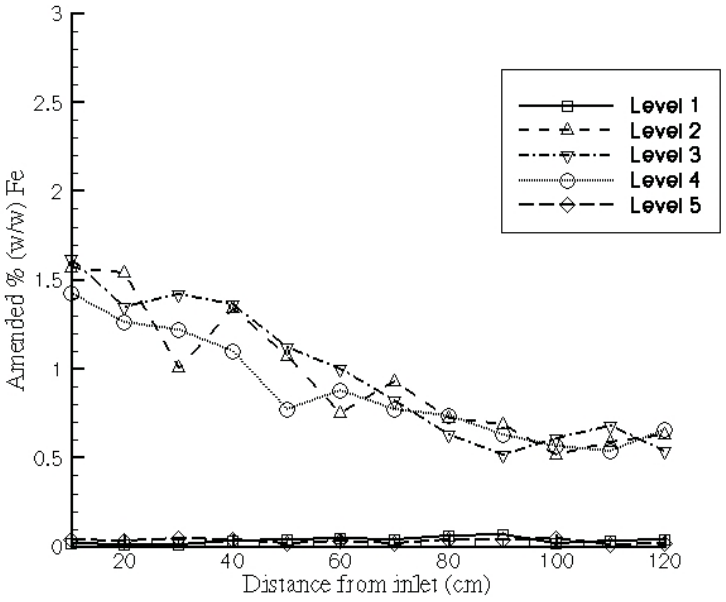

Figure 17. Amended % (w/w) Fe^0 at All Five Levels as a Function of Distance from Injection Location (Experiment 2)

Based on amended concentrations of 0.6% w/w zero-valent iron, barrier longevity calculations can be performed, similar to Szecsody et al. (2005). The longevity of a zone containing Fe^0 iron can be determined from the ratio of the iron in the sediments to the electron acceptors in the aquifer. The identified electron acceptors are dissolved oxygen (8 mg/L), nitrate (60 mg/L) and chromate (2 mg/L). Assuming a representative dry bulk density of 2300 kg/m^3, a porosity of 0.14 (Szecsody et al. 2005), and 3 moles of electrons per mole of iron, 0.6% Fe^0, with a molecular weight of 55.85 g/mol can donate $(0.006 \times 2300 \times 3/55.85) \times 1000 = 740$ mol e^-/m^3 of porous medium. Assuming that oxygen (molecular weight: 32 g/mol) accepts 4 mol e^-/mol, nitrate (molecular weight: 62 g/mol) 2 mol e^-/mol, and chromate (molecular weight 117 g/mol) 3 mol e-/mol, a unit volume of porous medium with a saturated porosity of 0.14 is able to accept $(8 \times 4/32 + 60 \times 2/62 + 2 \times 3/117) \times 140/1000 = 0.28$ mol e^-. The ratio of 740/0.28 indicates that 2640 pore volumes of ground water have to flow through a treated zone before breakthrough is observed. The longevity of a zero-valent iron barrier with length p m (p/0.305 ft) and groundwater velocity of k m/day (k/0.305 ft/day) is $(2640 \times p)/(365.25 \times k)$ years. For instance, a 1 m Fe^0 amended zone with an average concentration of 0.6% w/w iron subject to a pore water velocity of 1 m/day will have longevity of 7.2 years.

4.0 Summary

At the Hanford Site, a field-scale ISRM barrier was installed to prevent chromate from reaching the Columbia River. However, chromium has been detected in several wells, indicating premature loss of reductive capacity in the aquifer. One possible cause for premature chromate breakthrough is associated with the presence of high-permeability zones in the aquifer. In these zones, groundwater moves relatively faster and is able to oxidize iron more rapidly. It is also possible that the high-permeability flow paths may be deficient in reducing equivalents (e.g., reactive iron), which is required for barrier performance.

One way enhancement of the current barrier reductive capacity can be achieved is by the addition of micron-scale zero-valent iron (DOE 2004a). The potential emplacement of zero-valent iron into high-permeability Ringold Unit E gravels using shear-thinning fluids containing polymers was investigated in three-dimensional wedge-shaped aquifer models. The primary reason for using polymers was to create a suspension that is both viscous enough to keep the Fe^0 in solution for extended time periods, improving colloid movement into the porous media, while not causing a detrimental decrease in hydraulic conductivity. Porous media were packed in the wedge-shaped flow cell to create either a heterogeneous layered system with a high-permeability zone between two low-permeability zones or a high-permeability channel surrounded by low-permeability materials. The injection flow rate, polymer type, polymer concentration, and injected pore volumes were determined based on a series of preliminary short- and long-column experiments.

The flow cell experiments indicate that iron concentration enhancements of at least 0.6% (w/w) could be obtained using moderate flow rates and injection of 30 pore volumes. Although the aqueous pressure increased by up to 25 KPa (~3.5 psi) during infiltration, a detrimental effect to the hydraulic conductivity was not observed.

Calculations show that the longevity of a 0.6% amended zero-valent iron zone will provide 2640 pore volumes of treatment before breakthrough is observed, assuming groundwater flowing through the treatment zone contains 8 mg/L oxygen, 60 mg/L nitrate, and 2 mg/L chromate, and assuming a complete reduction of these redox-reactive species. For instance, a 1-m-long Fe^0 amended zone with an average concentration of 0.6% w/w iron subject to a groundwater velocity of 1 m/day will have an estimated longevity of 7.2 years. To provide an example of comparable scale to that which would be required at the 100-D Area ISRM barrier site, a 10-m-long amended zone with an average concentration of 0.6 w/w % zero-valent iron subject to a typical 100-D Area groundwater velocity of 0.3 m/day would have an estimated longevity of 240 years. The 0.6% amended Fe^0 concentration would provide approximately 20 times the average reductive capacity that is provided by the dithionite-reduced Fe(II) in the ISRM barrier.

The flow cell experiments conducted in this study indicated that in the downstream half of the flow cell the iron concentration stabilizes at about 0.6 % (w/w). These results suggest that additional research is needed in longer intermediate-scale flow cells to investigate how far from

the injection well considerable iron enhancements can be obtained. For effective supplemental treatment of the 100-D Area ISRM barrier, a radial extent of treatment of approximately 5 to 7 m would be required. Flow cell experiments are also needed to provide direct measurement of the longevity of high-permeability zones amended with zero-valent iron. In these experiments, groundwater with representative dissolved oxygen, nitrate, and chromate concentrations would be allowed to move through the amended zones. Through sampling at various locations, oxygen, nitrate, and chromium concentration data would be collected. Results from these experiments should be compared with results from longevity calculations presented in this report. These experiments would also be useful for determining how groundwater displaces the emplaced viscous polymer solutions and to study how the injected polymer degrades over time.

5.0 References

Cantrell KJ and DI Kaplan. 1997. "Zero-valent iron colloid emplacement in sand columns." *J. Env. Eng*., 123:499-505.

Cantrell KJ, DI Kaplan, and TJ Gilmore. 1997a. "Injection of colloidal size particles of Fe^0 in porous media with shear thinning fluids as a method to emplace a permeable reactive zone." *Land Contamination and Reclamation,* 5:253-257.

Cantrell KJ, DI Kaplan, and TJ Gilmore. 1997b. "Injection of colloidal Fe^0 particles in sand with shear-thinning fluids." *J. Env. Eng*., 123:786-791.

FHI. 2005. In Situ Redox Manipulation First Quarter Fiscal Year 2005 Technical Memorandum. MP-25950 Rev. 0, Fluor Hanford Inc., Richland, Washington.

Fruchter JS, C Cole, MD Williams, VR Vermeul, J Amonette, JE Szecsody, J Istok, and M Humphrey. 2000. "Creation of a Subsurface Permeable Treatment Barrier Using In-Situ Redox Manipulation." *Ground-Water Monitoring Review*, 66–77.

Gillham RW and SF O'Hannesin. 1994. "Enhanced degradation of halogenated aliphatics by zero valent iron." *Ground Water,* 32:958-967.

Kaplan DI, KJ Cantrell, and TW Wietsma. 1994. "Formation of a barrier to groundwater contaminants by the injection of zero-valent iron colloids: suspension properties." *In-situ remediation: scientific basis for current and future technologies,* GW Gee and NR Wing, eds.. Battelle Press, Columbus, Ohio, pp. 820-838.

Kaplan DI, KJ Cantrell, TW Wietsma, and MA Potter. 1996. "Retention of zero-valent iron colloids by sand columns: Application to chemical barrier formation." *J. of Environmental Quality*, 25:1086-1094.

Klute A and C Dirksen. 1986. "Hydraulic conductivity and diffusivity: laboratory methods. *Methods of soil analysis. Part 1. Agron. Mono. 9,* A. Klute (ed.). ASA and SSSA, Madison, Wisconsin, pp. 687-734.

Kostarelos K, GA Pope, BA Rouse, and GM Shook. 1998. "A new concept: the use of neutrally buoyant microemulsions for DNAPL remediation." *J. of Contam. Hydrol*., 34:383-397.

Lake LW. 1989. *Enhanced Oil Recovery*. Prentice Hall, Englewood Cliffs, New Jersey.

Martel KE, R Martel, R Lefebvre, and PJ Gelinas. 1998. "Laboratory study of polymer solutions used for mobility control during in situ NAPL recovery." *Ground Water Monitoring and Remediation*, 25:103-113.

Schroth MH, SJ Ahearn, JS Selker, and JD Istok. 1996. "Characterization of Miller-similar silica sands for laboratory hydrologic studies." *Soil Sci. Soc. Am. J.*, 60:1331-1339.

Szecsody JE, VR Vermeul, JS Fruchter, MD Williams, BJ Devary, JL Philips, M Rockhold, and Y Liu. 2005. *Effect of geochemical and physical heterogeneity on the Hanford 100D area in situ redox manipulation barrier longevity*. PNNL-15449, Pacific Northwest National Laboratory, Richland, Washington.

U.S. Department of Energy (DOE). 2004a. *Mending the in situ redox manipulation barrier*. Technical Assistance Project #28 Final Technical Solutions Report, DOE, Washington, D.C.

U.S. Department of Energy (DOE). 2004b. *Mending the in situ redox manipulation barrier.* Technical Assistance Project #33 Final Technical Solutions Report, DOE, Washington, D.C.

U.S. Department of Energy (DOE). 2005. *Fiscal Year 2004 Annual Summary Report for the In Situ Redox Manipulation Operations.* DOE/RL-2009-39, prepared by FHI for the DOE Richland Operations Office, Richland, Washington.

Vermeul VR, MD Williams, JE Szecsody, JS Fruchter, CR Cole, and JE Amonette. 2002. "Creation of a Subsurface." *Groundwater Remediation of Trace Metals, Radionuclides, and Nutrients, with Permeable Reactive Barriers.* Academic Press.

Williams MD, VR Vermeul, JE Szecsody, and JS Fruchter. 2000. *100-D Area in-situ redox treatability test for chromate-contaminated groundwater*. PNNL-13349, Pacific Northwest National Laboratory, Richland, Washington.

Appendix

Iron Concentrations for Experiments

Appendix - Iron Concentrations for Experiments

Table A.1. Amended Fe^0 Concentrations (% w/w) for Experiment 1

Sample Number	Level 1	Level 2	Level 3	Level 4	Level
1	0.05	0.04	0.08	0.07	0.06
2	0.04	0.04	0.06	0.04	0.06
3	0.07	0.64	0.50	0.70	0.04
4	0.07	0.62	0.49	0.74	0.12
5	0.08	0.60	0.60	0.71	0.07
6	0.09	0.66	0.62	0.73	0.06
7	0.09	0.63	0.49	0.72	0.08
8	0.04	0.05	0.06	0.07	0.06
9	0.00	0.06	0.08	0.07	0.10
10	0.05	0.07	0.06	0.06	0.09
11	0.05	0.04	0.09	0.07	0.09
12	0.03	0.63	0.63	0.55	0.11
13	0.03	0.62	0.73	0.53	0.12
14	0.02	0.55	0.68	0.67	0.04
15	0.06	0.56	0.69	0.64	0.07
16	0.05	0.59	0.67	0.59	0.11
17	0.05	0.07	0.06	0.06	0.09
18	0.04	0.08	0.04	0.04	0.10
19	0.03	0.06	0.08	0.03	0.11
20	0.04	0.52	0.61	0.66	0.12
21	0.03	0.55	0.60	0.62	0.08
22	0.05	0.49	0.62	0.76	0.07
23	0.05	0.47	0.55	0.64	0.07
24	0.04	0.57	0.67	0.72	0.09
25	0.04	0.07	0.08	0.07	0.09
26	0.06	0.05	0.06	0.05	0.04
27	0.07	0.65	0.50	0.66	0.08
28	0.06	0.74	0.55	0.72	0.06
29	0.08	0.70	0.56	0.62	0.07
30	0.04	0.54	0.47	0.60	0.05
31	0.04	0.82	0.52	0.50	0.05
32	0.08	0.05	0.07	0.07	0.07
33	0.05	0.07	0.06	0.05	0.02
34	0.07	0.75	0.65	0.80	0.06
35	0.06	0.70	0.67	0.81	0.05

Table A.1 (Contd)

Sample Number	Level 1	Level 2	Level 3	Level 4	Level
36	0.02	0.81	0.50	0.79	0.04
37	0.05	0.62	0.58	0.89	0.07
38	0.03	0.72	0.63	0.68	0.06
39	0.05	0.06	0.04	0.06	0.05
40	0.08	0.90	1.10	0.99	0.11
41	0.09	0.89	1.15	1.05	0.10
42	0.07	0.85	0.89	1.02	0.09
43	0.09	1.18	1.12	0.90	0.12
44	0.08	0.93	1.28	0.99	0.11
45	0.07	1.28	1.40	1.21	0.10
46	0.05	1.04	1.25	1.10	0.08
47	0.07	1.20	1.19	0.90	0.05
48	0.03	1.10	1.24	1.05	0.12
49	0.03	1.08	1.08	1.04	0.15
50	0.13	1.55	1.36	1.59	0.07
51	0.12	1.50	1.46	1.61	0.09
52	0.10	1.52	1.52	1.71	0.07
53	0.12	1.41	1.42	1.44	0.08
54	0.18	1.62	1.60	1.60	0.08
55	0.08	2.02	1.92	2.25	0.08
56	0.09	2.06	1.87	2.26	0.07
57	0.19	1.99	2.09	2.12	0.10
58	0.13	2.02	1.87	2.20	0.04
59	0.11	1.92	1.77	1.81	0.12
60	0.09	1.83	1.98	2.00	0.08
61	0.06	2.47	1.85	2.10	0.14
62	0.07	2.51	1.90	1.85	0.12
63	0.08	2.13	1.44	1.84	0.10
64	0.07	2.41	1.72	1.11	0.07

Table A.2. Amended Fe^0 Concentrations (% w/w) for Experiment 2

Sample Number	Level 1	Level 2	Level 3	Level 4	Level
1	0.04	0.63	0.54	0.66	0.02
2	0.03	0.55	0.50	0.60	0.03
3	0.02	0.59	0.55	0.61	0.03
4	0.05	0.71	0.70	0.71	0.00
5	0.05	0.53	0.46	0.58	0.01
6	0.03	0.66	0.53	0.69	0.03
7	0.03	0.67	0.50	0.66	0.02
8	0.04	0.73	0.48	0.77	0.02
9	0.06	0.60	0.60	0.66	0.01
10	0.03	0.55	0.60	0.53	0.00
11	0.02	0.52	0.62	0.50	0.02
12	0.04	0.64	0.64	0.46	0.00
13	0.02	0.66	0.67	0.60	0.01
14	0.04	0.55	0.73	0.61	0.01
15	0.03	0.52	0.77	0.54	0.00
16	0.04	0.67	0.69	0.52	0.03
17	0.02	0.50	0.72	0.57	0.00
18	0.04	0.70	0.71	0.55	0.01
19	0.00	0.52	0.66	0.57	0.03
20	0.00	0.61	0.68	0.60	0.03
21	0.04	0.60	0.61	0.63	0.08
22	0.04	0.44	0.65	0.60	0.07
23	0.02	0.47	0.45	0.41	0.04
24	0.01	0.52	0.60	0.61	0.05
25	0.03	0.48	0.62	0.56	0.04
26	0.07	0.73	0.55	0.60	0.04
27	0.04	0.72	0.58	0.62	0.00
28	0.08	0.75	0.60	0.66	0.02
29	0.08	0.60	0.62	0.64	0.06
30	0.04	0.64	0.45	0.55	0.07
31	0.10	0.69	0.40	0.71	0.05
32	0.08	0.70	0.45	0.63	0.04
33	0.06	0.70	0.71	0.72	0.04
34	0.04	0.79	0.63	0.71	0.04
35	0.04	0.75	0.65	0.68	0.05
36	0.05	0.72	0.67	0.69	0.03
37	0.07	0.66	0.69	0.90	0.01
38	0.07	0.60	0.53	0.78	0.07

Table A.2 (Contd)

Sample Number	Level 1	Level 2	Level 3	Level 4	Level
39	0.09	0.82	0.53	0.70	0.04
40	0.03	0.90	0.70	0.66	0.02
41	0.03	0.87	0.81	0.88	0.01
42	0.05	0.93	0.82	0.74	0.02
43	0.04	0.99	0.95	0.80	0.03
44	0.04	0.87	0.82	0.77	0.02
45	0.04	0.75	1.10	0.80	0.07
46	0.04	0.90	0.97	0.77	0.01
47	0.06	0.62	1.05	0.76	0.02
48	0.03	0.79	1.06	0.99	0.02
49	0.08	0.69	0.82	0.68	0.03
50	0.03	1.01	1.24	0.80	0.02
51	0.02	1.07	1.20	0.91	0.00
52	0.02	1.13	0.95	0.74	0.00
53	0.09	1.20	0.99	0.65	0.05
54	0.04	0.94	1.22	0.81	0.04
55	0.03	1.30	1.36	1.22	0.05
56	0.02	1.20	1.44	1.18	0.04
57	0.04	1.48	1.28	0.9	0.04
58	0.01	1.22	1.46	1.18	0.05
59	0.00	1.00	1.40	1.30	0.06
60	0.02	0.78	1.38	1.18	0.04
61	0.01	1.56	1.33	1.15	0.03
62	0.01	1.71	1.40	1.39	0.
63	0.02	1.35	1.32	1.24	0.
64	0.02	1.57	1.62	1.43.	0.04

Distribution

DOE Richland Operations Office

BL Charboneau
JG Morse
KM Thompson
AC Tortoso

Fluor Hanford, Inc.

JV Borghese
TW Fogwell
BH Ford
R Jackson
VG Johnson
SW Petersen
LC Swanson

Washington State Department of Ecology

J Price

Pacific Northwest National Laboratory

JE Amonette
BJ Devary
JS Fruchter
TJ Gilmore
Y Liu
JP McKinley
JL Phillips
ML Rockhold
JE Szecsody
VR Vermeul
MD Williams

Distribution will be made by email notification of availability from PNNL publication website (http://www.pnl.gov/main/publications/).